Research paper

Size evolution relativistic DFT-QTAIM study on the gold cluster complexes Au_4-S-C_nH_{2n}-S'-Au_4' (n=2-5)

Juan I. Rodríguez, Emilbus A. Uribe, María I. Baltazar-Méndez, Jochen Autschbach, F.L. Castillo-Alvarado, Israel Gutiérrez-González

PII: S0009-2614(16)30605-4
DOI: http://dx.doi.org/10.1016/j.cplett.2016.08.038
Reference: CPLETT 34097

To appear in: *Chemical Physics Letters*

Received Date: 16 July 2016
Revised Date: 14 August 2016
Accepted Date: 17 August 2016

Please cite this article as: J.I. Rodríguez, E.A. Uribe, M.I. Baltazar-Méndez, J. Autschbach, F.L. Castillo-Alvarado, I. Gutiérrez-González, Size evolution relativistic DFT-QTAIM study on the gold cluster complexes Au_4-S-C_nH_{2n}-S'-Au_4' (n=2-5), *Chemical Physics Letters* (2016), doi: http://dx.doi.org/10.1016/j.cplett.2016.08.038

Size evolution relativistic DFT-QTAIM study on the gold cluster complexes Au_4-S-C_nH_{2n}-S'-Au_4' (n=2-5)

Juan I. Rodríguez[1*], Emilbus A. Uribe[2], María I. Baltazar-Méndez[1], Jochen Autschbach[3], F.L. Castillo-Alvarado[1], and Israel Gutiérrez-González[4]

[1] *Escuela Superior de Física y Matemáticas, Instituto Politécnico Nacional, Edificio 9, U.P. A.L.M., Col. San Pedro Zacatenco, C.P. 07738, México D.F., México.*

[2] *Departamento de Ciencias Básicas, Universidad Santo Tomás, Carrera 9 No. 51-11, Bogotá, Colombia.*

[3] *Department of Chemistry, University at Buffalo, State University of New York, Buffalo, 14260-3000 New York, USA.*

[4] Unidad Académica Profesional Nezahualcóyotl, Universidad Autónoma del Estado de México, *Av. Bordo de Xochiaca s/n C.P. 57000, Ciudad Nezahualcóyotl, Edo. de México, México.*

ABSTRACT

We introduce relativistic density functional theory (DFT) calculations on the gold cluster complexes (cluster-molecule-cluster) Au_4-S-C_nH_{2n}-S'-Au_4' (n=2-5). The structural, electronic and relativistic (ZORA) Bader's quantum theory of atoms in molecules (QTAIM) properties of the two lowest-energy complex isomers were computed as a function of the alkanedithiol size (n). The lowest-energy isomer is a triplet spin state independently of the complex size. According to QTAIM, the Au-Au and S-Au bonds are classified as closed shell (non-covalent) type. The HOMO-LUMO gap of the cluster complexes shows a zigzag behavior typical of gold nanoclusters with respect to the size of the alkanedithiol chain (n).

* Corresponding author: jirodriguezh@ipn.mx

keywords: gold nanoclusters, alkanedithiols, DFT, QTAIM, molecular nanowires, molecular electronics

I. INTRODUCTION

Molecular electronics will be a commercial technology as long as every part of a circuit (wire, capacitor, inductor, battery, etc.) can be constructed with one or few molecules. [1-3] Molecular logic gates, rectifiers, transistors, motors, etc., could be then obtained from these building blocks. [3] Research on this interesting and challenging topic is ongoing. [1-5] As being made from one or few molecules, these molecular devices might lose their stability as an isolated entity (or their properties might change drastically) when interacting with the other devices and/or different environments. Thus they must be well characterized and tested *in vivo*. Currently, it is not always feasible to experimentally control them and measuring their properties due mainly to their nanometric size and/or weak bonding. [3-5] As in other research fields, computational simulations can be important tools for the characterization of these molecular devices.

Using a single molecule as a wire (conductor) has been the research topic of many experimental and theoretical works. [4-18] The system lead-molecule-lead has been theoretically modeled as cluster-molecule-cluster to: 1) make the calculations easier, 2) model part of the lead-cluster-molecule-cluster-lead array, and 3) estimate the use of the $(\text{cluster-molecule-cluster})_n$ ($n>1$) as the potential wire itself. [19-23] A dithiol linking two gold clusters (like the systems studied here) has been previously studied [19-22, 24-30] due to the special properties of gold nanoclusters and its preferential bonding with sulfur in self-assembled-monolayers and passivated gold nanoclusters by thiols. [31-32] The chemical bonding between sulfur and gold plays an important role as bridge between the organic and the "metallic" part. Yet, the precise nature of the chemical bonding between gold and sulfur in these

systems remains as a question to be answered. [31-33] This paper aims to shed some light on this direction.

In this work, we performed relativistic unrestricted Kohn-Sham DFT calculations for computing the structural, electronic, and QTAIM properties of the two lowest-energy isomers of the cluster complexes (see Figure 1 below) Au_4-S-C_nH_{2n}-S'-Au_4' (n=2-5). These properties are analyzed as a function of the size of the alkanedithiols (number of carbon atoms) in-the-complex. QTAIM analysis was performed for both computing the atomic properties and determining the chemical bonding mainly at the gold-thiol interface. The change on the alkanedithiol (gold cluster) properties (e.g. charge) in-the-complex with respect to the corresponding properties as an isolated molecule (gold cluster) was determined. One can thus quantitatively determine the influence of the "metallic" part (gold nanoclusters) on the organic part (alkanedithiol) properties in-the-complex and vice versa. It is worth mentioning that until recently the QTAIM properties had only been computed within the Bader's original non-relativistic formulation. [34] Recently, however, the scalar relativistic zeroth-order regular approximation (ZORA) extension of QTAIM was introduced [35] and computationally implemented/tested by us. [36] As for other properties, relativistic effects on the QTAIM properties are important for heavy atoms (like gold). [36] The QTAIM properties reported in this work for the cluster complexes Au_4-S-C_nH_{2n}-S'-Au_4' were computed at the relativistic ZORA level of theory (by the first time as far as we know for these systems). The remainder of the article is organized as follows: The computational details are introduced in Sec. II. Our results and conclusions are shared in Secs. III and IV, respectively.

II COMPUTATIONAL DETAILS

All calculations were performed with the Amsterdam Density Functional (ADF 2014) package. [37-39] A partial search the potential energy surface (PES) of the complexes Au_4-S-C_nH_{2n}-S'-Au_4' for each size

(n=2-5) was carried out. A family of at least 7 different nuclear geometries of each cluster complex were constructed to be used as initial structures in the geometry optimizations considering two different spin states (M=2S+1=1,3) in each case. The optimized structures of the isolated alkanedithiol (n=2-5) and two isomers (planar diamond and tetrahedral geometry) of Au_4 (see Figure 1 below) were used to construct the starting geometries for the complex optimizations changing the relative position of one gold atom of the Au_4 isomer and the sulfur atom in the thiols. The two lowest-energy isomers of each complexes Au_4-S-C_nH_{2n}-S'-Au_4' (n=2-5) obtained via this process are reported here. The geometries were fully optimized at the relativistic ZORA unrestricted DFT level of theory (ZORA-U-DFT), considering a convergence threshold for the energy gradients with respect to the nuclear coordinates equal to 10^{-3} Hartree/angstrom without using any molecular symmetry restriction. For the two lowest energy isomers of each complex size, n=2-5, (see Figure 1), an all-electron self consistent field (SCF) single point (SP) ZORA DFT calculation followed by a QTAIM calculation was performed at the optimized geometry. The relativistic ZORA-QTAIM calculations were performed using our ultrafast method as implemented in ADF [40-42]. For both geometry optimization and SP calculations, the (generalized-gradient-approximation) Perdew-Burke-Ernzerhof (PBE) [43] functional and a triple-ζ polarized Slater (TZP) basis set were used. [37-39] For the geometry optimization, the 1s-4f core has been kept frozen (FC) for Au atoms. Unless otherwise stated, the ADF default setting for the SCF, geometry optimization, and QTAIM property calculation procedure were used. [37-42]

III RESULTS AND DISCUSSION

A. Structural Properties

Figure 1 shows the optimized structure of the two lowest-energy isomers for each cluster complex size (n=2-5) along with the lowest-energy structure (planar diamond) of the isolated Au_4 , and the $C_2H_4S_2H_2$ as a representative Au_4 cluster and alkanedithiol. In order to understand the scope of our

approximations, let us first compare our data with previous calculations are available. There is a consensus on the planar diamond (trapezoid) as the lowest-energy structure of Au_4 (see Figure 1(a)). From Figure 1 we can see that average Au-Au bond distance obtained at our level of theory (UPBE-TZP-ZORA-FC) for Au4 is equal to 2.7006Å, which is good agreement with the one reported by Basch and Ratner (2.7324Å, at the UB3LYP-SKBJ-relativistic pseudopotential level) and Fernandez *et al*. (2.69Å, at the PBE-DZ-relativistic pseudopotential level), which represent a 1.1% and 0.4% difference, respectively, with respect to our value. [20,44] The S-H and S-C bond distance in isolated $C_2H_4S_2H_2$ (see Figure 1(a)) computed by us are equal to l.359Å and 1.848Å, respectively, which are also in good agreement with the corresponding values reported by Basch and Ratner (1.362Å and 1.855Å), which represent a 0.2% and 0.4% difference, respectively. [20] As for the cluster complexes, as far as we know, there is only previous data for the complex Au_4-S-C_2H_4-S'-Au_4' (n=2), which was reported by Basch and Ratner. The two lowest-energy isomers of Au_4-S-C_2H_4-S'-Au_4' found by us (see Figure 1(b)) are basically those reported by them. However, they reported the Isomer 1 in the spin state M=1 (singlet) while we found that this state is 0.1eV higher in energy than the state M=3 (triplet). Actually we found that the spin state M=3 is the lowest energy state for each isomer in all cases, which can be seen in Figure 1(b)-(f). Only the properties of these lowest-energy (triplet) isomers are reported here. The type of bonding between sulfur and gold atoms (S-Au(i)) in these isomers (n=2, Figure 1(b)) is depicted in the diagram of Figure 2(i). Sulfur is bonded to two gold atoms of different bond distance (2.43Å and 2.37Å). As can be seen in Figure 1(b) (see also Table 3), differences between the equivalent "large" bonds (2.43Å) attached to both sides (Au_4 and Au_4') is in the 3rd decimal place for both isomers; differences between "short" bonds are also in the 3rd decimal except for the bond attached to Au_4 of Isomer 1, for which the difference is in the 2nd decimal place with respect to all other equivalent short bonds (see also Table 2). As can be seen in Figure 1(b), the S-C and S-C' bond distances are different in Isomer 1 (1.861Å and 1.859Å, respectively) and equal in Isomer 2 (1.861Å).

The maximum difference between our bond distance value (Isomer 1) and the corresponding ones reported by Basch and Ratner is equal to 2.4% (with respect to their M=3 isomer for which the S-C and S-C' bond distances are different). [20] Thus our data obtained (at the U-PBE-TZP-ZORA level of theory) is in relatively good agreement with previous calculations. [20]

The optimized structure of the two lowest-energy isomers for the larger cluster complexes (n=3-5) can be seen in Figure 1(c)-(e), which show a more interesting variety of the sulfur-gold bonding. The diagram of the bonding types between sulfur and gold can be seen in Figure 2. Isomer 1 of the complex Au_4-S-C_3H_6-S'-Au_4' (n=3) exhibit the S-Au(i) bonding in the left side (Au_4) and the S-Au(ii) in the right side (Au_4') (see Figure 1(c)). The left side bonding S-Au(i) is similar to one discussed above for Au_4-S-C_2H_4-S'-Au_4' (n=2). The main differences between isomers 1 for n=2 and n=3 are: i) the Au-S-C angle which is sharper ($99°$) for the complex Au_4-S-C_3H_6-S'-Au_4' (n=3) than the one ($104.3°$) for Au_4-S-C_2H_4-S'-Au_4' (n=2); ii) the S-Au short (large) bond is a bit longer, 0.06Å, (shorter, 0.018Å) in Au_4-S-C_3H_6-S'-Au_4' (n=3) than the corresponding ones in Au_4-S-C_2H_4-S'-Au_4' (n=2), which can be seen clearly from Figure 1(b)-(c) (see also Table 3). The right hand side bonding is of the type S-Au(ii) in Isomer 1 of Au_4-S-C_3H_6-S'-Au_4' (n=3), where Au_4' is in a tetrahedral geometry (see Figure 1(c)). In this bonding type sulfur forms only one bond with gold. The bond distance of the S-Au bond is equal to 2.288A, which is shorter than the double bond (2.372Å) of the S-Au(ii) type. A similar type of bond has been reported for anion benzene dithiol (2.366Å) and alkene dithiols (2.389Å) but not for neutral complex (see Reference 21). From Figure 1(d), notice that for Isomer 2 of Au_4-S-C_4H_8-S'-Au_4' (n=4), the S-Au bonding is of the same type S-Au(ii) for both sides (both Au_4 and Au_4' have tetrahedral geometry) with almost the same bond distance (2.27Å and 2.271Å, respectively). This structure is interesting since it is quite similar to the structure of an isolated alkane (see Figure 1(a)) where each ending hydrogen atom is replaced by one Au_4 nanoparticle (superatom). The Au-S-C angle for this S-

Au(ii) bond is about 105° in all cases (see Figure 1(c)-(f)). The third different type of S-Au bonding (iii) can been seen in Isomer 2 of the complex Au_4-S-C_5H_{10}-S'-Au_4' (n=5) (see Figure 1(e)). Sulfur forms also only one bond with Au (in Au_4), however, Au_4 in this case has planar diamond (trapezoid) geometry. The gold atom that participates in the S-Au(iii) bond is one on the trapezoid minor axis. The S-Au bond distance is equal to 2.277Å for this S-Au(iii) bonding. Notice that the S-Au bond formed with Au_4' is of the S-Au(ii) type with the shortest S-Au bond distance (2.269Å). Isomer 2 of Au_4-S-C_3H_6-S'-Au_4' (n=3) is a special case (see Figure 1(c)). Interestingly, in this complex although sulfur (S) is bonded to two gold atoms of Au_4 (planar diamond) via almost equivalent double bonds (2.32Å and 2.37Å), its bond with carbon is broken forming a thiolate (see Figure 2(iv)). The Bader charge of this sulfur atom is equal to -0.254a.u. (see Table 3 below and the related discussion). The carbon atom that was bonded to S now gets bounded to one gold atom on the minor axis of the trapezoid Au_4 nanocluster (see Figure 1(c)) making the bridge between the alkane chain and Au_4 nanocluster. The C-Au bond distance and C-Au-S angle are equal to 2.108Å and 94°, respectively (see next subsection).

B. QTAIM (Bader) Properties

Figure 3 shows the molecular graphs of the cluster complexes (b)-(e) along with the ones for isolated Au_4 and $C_2H_4S_2H_2$ (a). These are the corresponding molecular graphs for the structures shown in Figure 1. Tables 1-3 show the bond information for the isolated systems (Au_4 and $C_2H_4S_2H_2$) and the cluster complexes. According to QTAIM, there is a bond critical point (BCP) of the electron density between any pair of chemically bonded atoms in a molecule (cluster or solid). [34] A general and interesting trend we found for the S-Au(i) bonding type (see Figure 2) is that there is not a chemical bond between the two gold atoms that participate in it, since there is not a BCP between such Au atoms (see Figure 3(b)-(e)). Thus, according to QTAIM, when sulfur gets bonded to two gold atoms via a S-Au(i) bonding type, the original bond between these two Au atoms, which can be seen is predicted by

the existence of a BCP in isolated Au_4 (see Figure 3(a)), is broken. However, notice that the standard software molecule viewer used to get the 3-dimensional structure of the complexes in Figure 1(b)-(e) put a stick between these pair of Au atoms, which is based solely on distance criteria and should not be mistaken for a bond unless an electronic structure analysis confirms the existence of a bond1. As can be seen from Figure 1(b)-(e), the Au-Au distance between these two Au atoms linked to S is greater than 3Å. This distance is greater than the average first neighbour distance reported for gold nanoclusters which is typically in the range 2.6-2.84Å (see for instance Figure 1(a)), it is even greater than the average first neighbour distance in bulk gold (2.88Å). [45-46] From Figure 3(b)-(e), we can also see that these two Au atoms involved in the S-Au(i) bonding type are also linked to another Au atom in Au_4. Thus these three Au atoms along with S form a ring which is confirmed by the existence of a ring critical point (RCP) as can be seen in green in Figure 3(b)-(e).

Table 3 shows the bond information for the S-Au interface organized according to the bonding classification of Figure 2. Notice that there is general correlation between the bonding type and the bond information (charge, ρ,$\nabla^2\rho$ and bond distance R_e). Equivalent S-Au bonds have (approximattely) the same bond information independently of the size of the cluster complex (see Table 3). In the S-Au(i) bonding type, S (Au) gets negativelly (positivelly) charged forming an electrostatic dipole moment. This dipole is greater for the shorter bond as could be expected, the positive charge of Au is almost one order of magnitud greater in the shorter bond (~0.1a.u) than in larger bond (~ 0.037a.u. in average). There is an exception to this rule which happens for Isomer 1 of Au_4-S-C_3H_6-S'-Au_4', in which sulfur has a small positive charge (0.01a.u.) and gold a negative charge (-0.041a.u) (see Table 3). The reason of this exception is because, interestingly, in this system S gets also bonded to the S', that is, a S-S' bond is formed which is predicted by the BCP between S and S' (see Figure 3(c)). The bond

1 The molecule viewer software usually use a purely geometric criterion putting a stick between two particular type of atoms if the distance between them is in a specific interval.

distance for this S-S' bond is equal to 2.731Å (see Table 2) which is actually in the range (2.729Å-2.886Å) of the theoretical values reported for the S-S bond in $H_2S\backslash SH_2^+$ [47].[2] In S-Au(ii) bonding type, S and Au form also a dipole moment but S gets a larger negative charge (~ -0.1a.u) and Au a smaller charge (~ 0.09a.u) with respect to the shorter bond of S-Au(i) bonding type. The bond information is similar for all bond in this S-Au(ii) bonding type except for the S'-Au' bond in which S' is the one that is involved in the S-S' bond in Isomer 1 of Au_4-S-C_3H_6-S'-Au_4' (see Figure 3(c) and Table 3). The S-Au bond distance in S-Au(ii) bonding type is in the range 2.269-2.288Å which is shorter than the shortest bond distance (2.320Å) of the S-Au bonds in S-Au(i) bonding type (see Table 3). In the contrary, the density value at the corresponing BCP of the S-Au bond in S-Au(ii) is greater that any corresponing value of the S-Au(i) bonding type. All these S-Au bonds are formed between sulfur and one atom in Au_4 in its tetrahedral geometry (see Figures 1 and 3), which forms a closed geometrical region as predicted by the existence of a cage critical point (CCP, in blue in Figure 3(c)-(e)). The S-Au bond in the S-Au(iii) bonding type has bond information quite similar to the short S-Au bond of S-Au(i) bonding type and, as expected, a bond distance (2.277Å), ρ and its Laplacian values, similar to the one of the S-Au(ii) bonding type (in both bonding types sulfur forms only one bond with Au, see Figure 2-3). As for the S-Au bond in the S-Au(iv) bonding type (Isomer 2 of Au_4-S-C_3H_6-S'-Au_4'), in which the S-C bond is broken (see Figures 1(c), 2(iv), 3(c)) the charge of S (-0.25) is quite larger than in all other S-Au bonds. In this case, as discussed above, one ending carbon atom of the alkane chain is bonded to one Au of Au_4 as predicted for the corresponding BCP. The C-Au bond distance is equal to 2.3Å which is similar to the theoretical value reported (2.01Å) for C-Au bonds in the systems Au20vNB and Au20vNB3 (NB: nitrobenzene). [48]

2 Notice that the molecule viewer software in this case does not put an stick to represent the S-S' bond in Figure 1 (see also footnote 1).

From Tables 1-2, notice that the value of the electron density (ρ) is less than 0.065a.u. and its Laplacian is positive ($\nabla^2\rho > 0$), at the BCP of all Au-Au bonds. The positive value of the Laplacian at the BCP's indicates a depletion of the density. Thus, according to QTAIM, the Au-Au bond is a closed shell (non-covalent) type in both isolated Au_4 and in any cluster complex. The Laplacian electron density at the BCP for the S-Au bond is also positive. Thus, in principle, the S-Au bonds are also closed shell type. However, it is expected that these S-Au bonds have also some electrostatic character due to the dipole moment formed between S and Au (see Bader charges in Table 3 and related discussion above), which was predicted before by Pakiari and Jamshidi [49]. According to the values of the density ρ and its Laplacian at the corresponding S-Au BCPs (see Table 3 and the discussion above), which are in agreement previous calculations [49], the S-Au(i) has the highest bond softening degree of these four bonding types, [50] which means that it is the weakest bond. The S-Au(ii) bonding type has the lowest bond softening degree, which means that this type of bond is the strongest one. [50] The bond softening degree for bonding types (iv) and (iii) are between these two limits.

C. Electronic Properties

Table 4 shows some electronic properties of the cluster complexes along with the ones for the isolated systems. As we can see from Table 4, the two isomers for the complex Au_4-S-C_2H_4-S'-Au_4' (n=2) are quasi-degenerated in energy. Their difference in energy is equal to 0.001eV. It is worth mentioning that we performed additional geometry optimizations for these two isomers considering a convergence threshold for the energy gradients with respect to the nuclear coordinates equal to 10^{-5} Hartree/angstrom. However, the small difference in energy (0.001) between these isomers holds. After a structural analysis we concluded that they are actually two different isomers with almost the same

energy. Figure 4 shows the dependence of the HOMO-LUMO gap (E_{HL}) with respect to the number of carbon atoms in the alkane chain (n) in the cluster complex. As we can see from Figure 4, E_{HL} shows a zigzag behavior typical for nanoclusters particularly for gold nanoclusters. The value of the HOMO-LUMO gap is between 0.5 and 1.2 eV, which is also the typical values of small gold nanoclusters, like for isolated Au_4 for which E_{HL} =0.99eV (see Table 4). [45-46] In the contrary, the HOMO-LUMO gap of the isolated alkanedithiols grows quasi-steadily with *n* from 4.38eV (n=2) to (4.78eV) as can be seen from Table 4. Notice the large value of E_{HL} for these organic molecules. Thus we could conclude that the cluster complexes Au_4-S-C_nH_{2n}-S'-Au_4' (n=2-5) as a whole behave like nanoclusters rather than organic molecules, at least as the HOMO-LUMO gap concerns (the part that is "growing" in the cluster complexes is the organic part though).

IV CONCLUSIONS

We have performed relativistic unrestricted Kohn-Sham DFT calculations for computing the structural, electronic, and QTAIM properties of the two lowest-energy isomers of the cluster complexes Au_4-S-C_nH_{2n}-S'-Au_4' (n=2-5). These properties are analyzed as a function of the size of the alkanedithiols (number of carbon atoms) in-the-complex. We found three types of bonding between sulfur and gold in these complexes in partial agreement with previous calculations. According to QTAIM, it was determined that the S-Au bonds can be classified as closed shell interaction. It was determined that the carbon in the alkane chain can form a bond with a gold atom in the Au_4 nanocluster. The dependence of the HOMO-LUMO gap with respect to the number of carbon atoms in-the-complex (n) shows a zigzag behavior typical of gold nanoclusters. Thus the complex as a whole might behave like a nano "particle" better than a molecule.

ACKNOWLEDGMENTS

JIR would like to thank SIP-IPN for financial support (project # 20161594) and UC-MEXUS-CONACYT (15-1462). EAU thanks Universidad Santo Tomás (Projects FODEIN 2015: Código 110000101-004 y Centro de Costos 17250556, and FODEIN 2016: Código: 1601512-002 y Centro de Costos 17250561) for the financial support. JA acknowledges support from the National Science Foundation, grant CHE-1265833.

REFERENCES

1. R. M. Metzger, Chem. Rev. 115, 5056 (2015).

2. L. Sun, Y. A. Diaz-Fernandez, T. A. Gschneidter, F. Westerlund, S. Lara-Avila, K. Moth-Poulsen, Chem. Rev. Soc. 43, 7378 (2014).

3. M. Ratner, Nature Nanotechnology 8, 378 (2013).

4. J. R. Heath, M. A. Ratner, Physics Today 56, 43 (2003).

5. S. V.Aradhya, L. Venkataraman, Nature Nanotechnology 8, 399 (2013).

6. E. Lörtscher, Nature Nanotechnology 8, 381 (2013).

7. A. Nitzan, M. A. Ratner, Science 300, 1384 (2003).

8 . Z.-Q. Fan, Z.-H. Zhang, W. Tian, X.-Q. Deng, G.-P. Tang, F. Xie, Org. Electron. 14, 2705 (2013).

9. J. Heurich, J. C. Cuevas, W. Wenzel, and G. Schön, Phys. Rev. Lett. 88, 256803 (2002).

10. J. Li,O. F. Sankey, Phys. Rev. Lett., 93, 248302 (2004).

11. R. Baer, D. Neuhauser, Int. J. Quantum. Chem. 91, 532 (2003).

12. M. Brandbyge, J.-L. Mozos, P. Ordejón, J. Taylor, K. Stokbro, Phys. Rev. B 65, 165401 (2002).

13. P. S. Damle, A. W. Ghosh, S. Datta, Phys. Rev. B 64, 201403 (2001).

14. P. A. Derosa, J. M. Seminario, J. Phys. Chem. B 105, 471 (2001).

15. E. G. Emberly, G. Kirczenow, Ann. N.Y. Acad. Sci. 960, 131 (2002).

16. E. G. Emberly, G. Kirczenow, Phys. Rev. B 61, 5740 (2000).

17. J. M. Seminario, C. E. De La Cruz, P. A. Derosa, J. Am. Chem. Soc. 123, 5616 (2001).

18. M. Di Ventra, S. T. Pantelides, N. D. Lang, Phys. Rev. Lett. 88, 046801 (2002).

19. K. Stokbro, J. Taylor, M. Brandbyge, J.-L. Mozos, P. Ordejón, Comp. Mat. Sci. 27, 151 (2003).

20. H. Basch, M. Ratner, J. Chem. Phys. 119, 11926 (2003).

21. H. Basch, M. Ratner, J. Chem. Phys. 119, 11943 (2003).

22. H. Basch, M. Ratner, J. Chem. Phys. 120, 5761 (2004).

23. C. W. Bauschlicher Jr., J. W. Lawson, A. Ricca, Y. Xue, M.A. Ratner, Chem. Phys. Lett. 388, 427 (2004).

24. A. Sen, C.-C. Kaun, ACS Nano 4, 6404 (2010).

25. J. R. Niskala, W. C. Rice, R. C. Bruce, T. J. Merkel, F. Tsui, W. You, J. Am. Chem. Soc. 134, 12072 (2012).

26. C. Li,I. Pobelov, T. Wandlowski, A. Bagrets ,A. Arnold, F. Evers, J. Am. Chem. Soc. 130, 318 (2008).

27. H. Bash,R. Cohen, M. A. Ratner, Nano Lett. 5, 1668 (2005).

28. R. B. Pontes, A. R. Rocha, S. Sanvito, A. Fazzio, A. J. Roque da Silva, ACS Nano 5, 795 (2011).

29. N. Sergueev, L. Tsetseris, K. Varga, S. Pantelides, Phys. Rev. B 82, 073106 (2010).

30. M. Strange, C. Rostgaard, H. Häkkinen, K. S. Thygesen, Phys. Rev. B 83, 115108 (2011).

31. H. Hakkinen, Nature Chemistry, 4, 443 (2012).

32. E. Pensa, E. Cortés, G. Corthey, P. Carro, C. Vericat, M. H. Fonticelli, G. Benítez, A. A. Rubert, R. C. Salvarezza, Acc. Chem. Res. 45, 1183 (2012).

33. F. P. Cometto, P. Paredes-Olivera,V. A. Macagno, E. M. Patrito, J. Phys. Chem. B 109, 21737 (2005).

34. R. F.W. Bader, "Atoms in Molecules: A Quantum Theory", Clarendon Press, Oxford (1990).

35. J. S. M. Anderson, P. W. Ayers, J. Phys. Chem. A 115, 13001 (2011).

36. J. S. W. Anderson, J. I. Rodríguez, P. W. Ayers, A. Goetz, J. Comp. Chem. (submitted).

37. E. J. Baerends, J. Autschbach, J. A. Berger, et al. ADF 2014, SCM, Theoretical Chemistry, Vrije Universiteit, Amsterdam, The Netherlands. 2014.

38. C. F. Guerra, J. G. Snijders, G. te Velde, E. J. Baerends, Theor. Chem. Acc. 99, 391 (1998).

39. G. te Velde, F. M. Bickelhaupt, S. J. A. van Gisbergen, C. Fonseca Guerra, E. J. Baerends, J. G. Snijders, T. Ziegler, J. Comput. Chem. 22, 931 (2001).

40. J. I. Rodríguez, R. F. W. Bader, P. W. Ayers, C. Michel, A. Goetz, C. Bo, Chem. Phys. Lett. 472, 149 (2009).

41. J. I. Rodríguez, P. W. Ayers, A. Goetz, F. de L. Castillo-Alvarado, J. Chem. Phys. 131, 021101 (2009).

42. J. I. Rodríguez, J. Autschbach, F.L. Castillo-Alvarado, M. I. Baltazar-Méndez, J. Chem. Phys. 135, 034109 (2011).

43. J. P. Perdew, K. Burke, M. Ernzerhof, Phys. Rev. Lett. 77, 3865 (1996).

44. E. M. Fernández, J. M. Soler, L. C. Bálbas, Phys, Rev. B 73, 235433 (2006).

45. M. C. Daniel D. Astruc, Chem. Rev. 104, 293 (2004).

46. H. Hakkinen,I. Landman, Phys. Rev. B 62, R2287 (2000).

47. F. M. Bickelhaupt, A. Diefenbach, S. P. de Visser, L. J. de Koning, N. M. M. Nibbering, J. Phys. Chem. A 102, 9549 (1998).

48. L. Laurentius, S. R. Stoyanov, S. Gusarov, A. Kovalenko, R. Du, G. P. Lopinski, M. T. McDermott. ACS Nano 5, 4219 (2011).

49.- A. H. Pakiari and Z. Jamshidi, J. Phys. Chem. A 114, 9212 (2010).

50. E. Espinosa, I. Alkorta, J. Elguero, E. Molins, J. Chem. Phys. 117 (2002) 5529.

FIGURES

Figure 1. Optimized structures of the lowest-energy isomers of (a) isolated systems ($C_2H_4S_2H_2$ and Au_4) and cluster complexes Au_4-S-C_nH_{2n}-S'-Au_4' for (b) n=2, (c) n=3, (d) n=4, and (e) n=5 carbon atoms. The bond distances are shown in angstroms (Å) and angles in degrees. The energies (eV) are also shown.

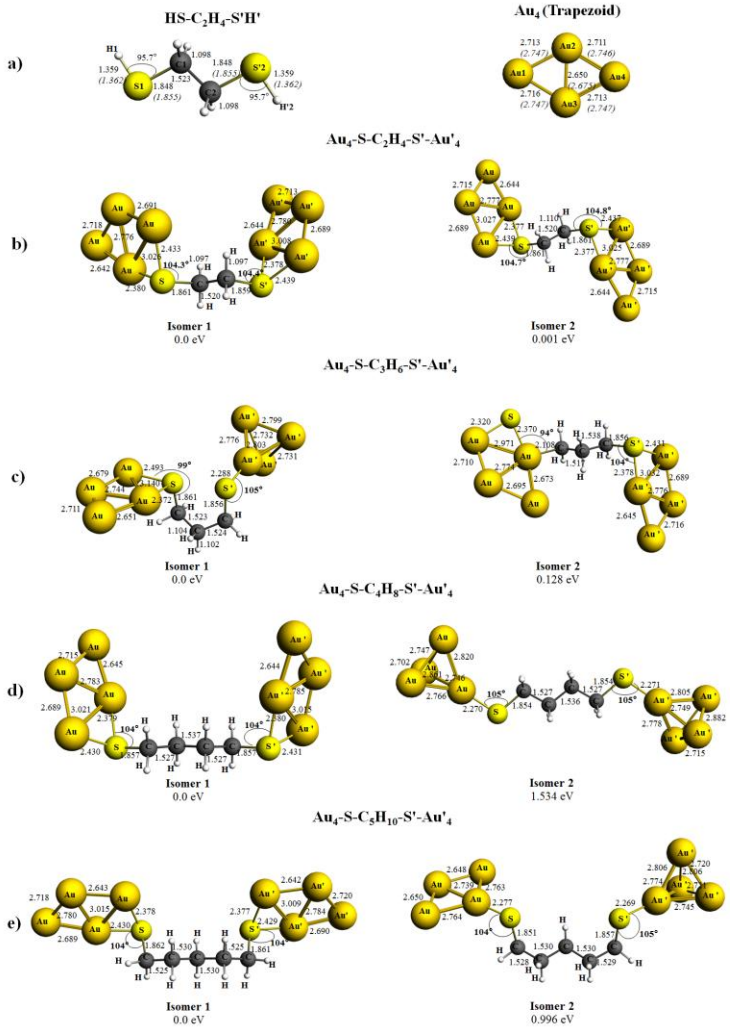

Figure 2. Types of bonding between S-C_nH_{2n}-S' (n=2-5) molecule and gold clusters (Au_4 and Au_4')

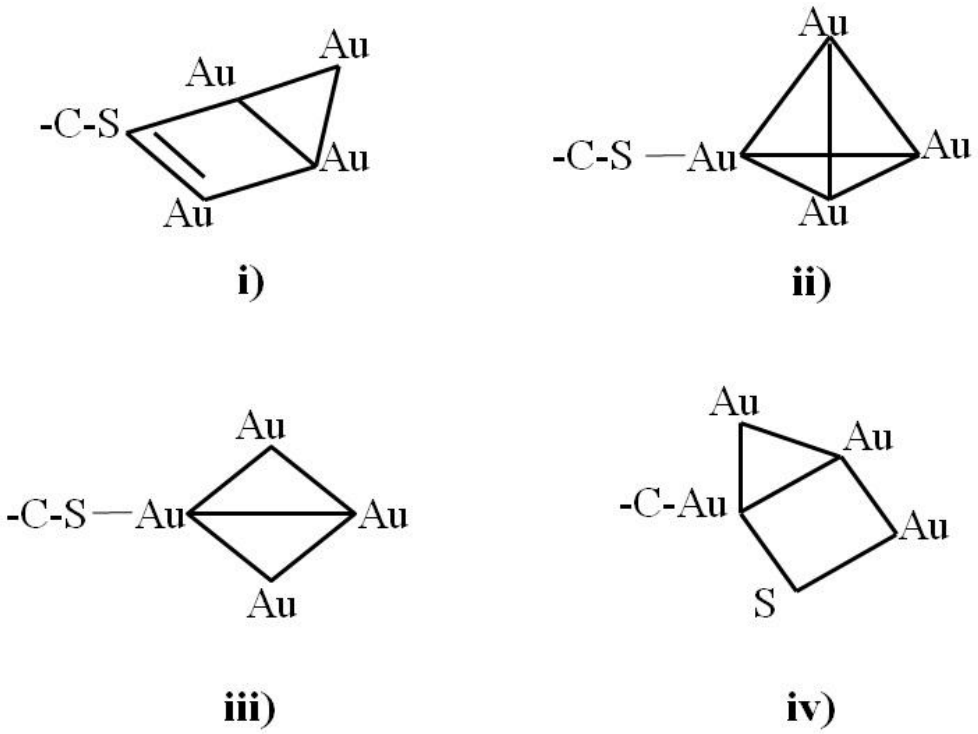

Figure 3. Molecular graphs for the structures shown in Figure 1. Nuclear critical points (NCP), bond critical points (BCP), and ring critical points (RCP) are in grey, red and green, respectively.

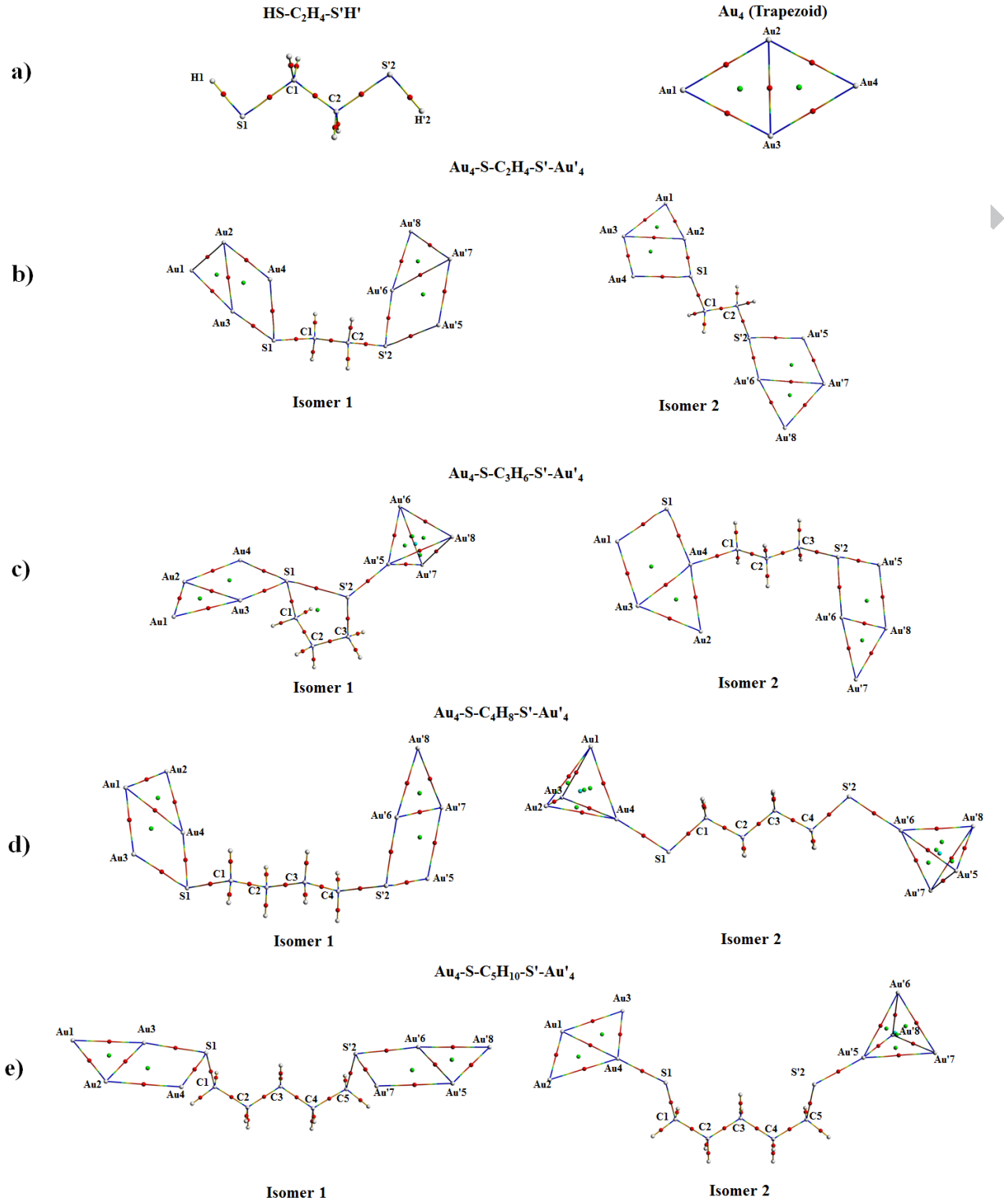

Figure 4. HOMO-LUMO gap (E_{HL}) of the cluster complexes Au_4-S-C_nH_{2n}-S'-Au_4' as a function of the number of carbon atoms in the alkane chain (n) for Isomer 1 group (solid line) and Isomer 2 group (dotted line).

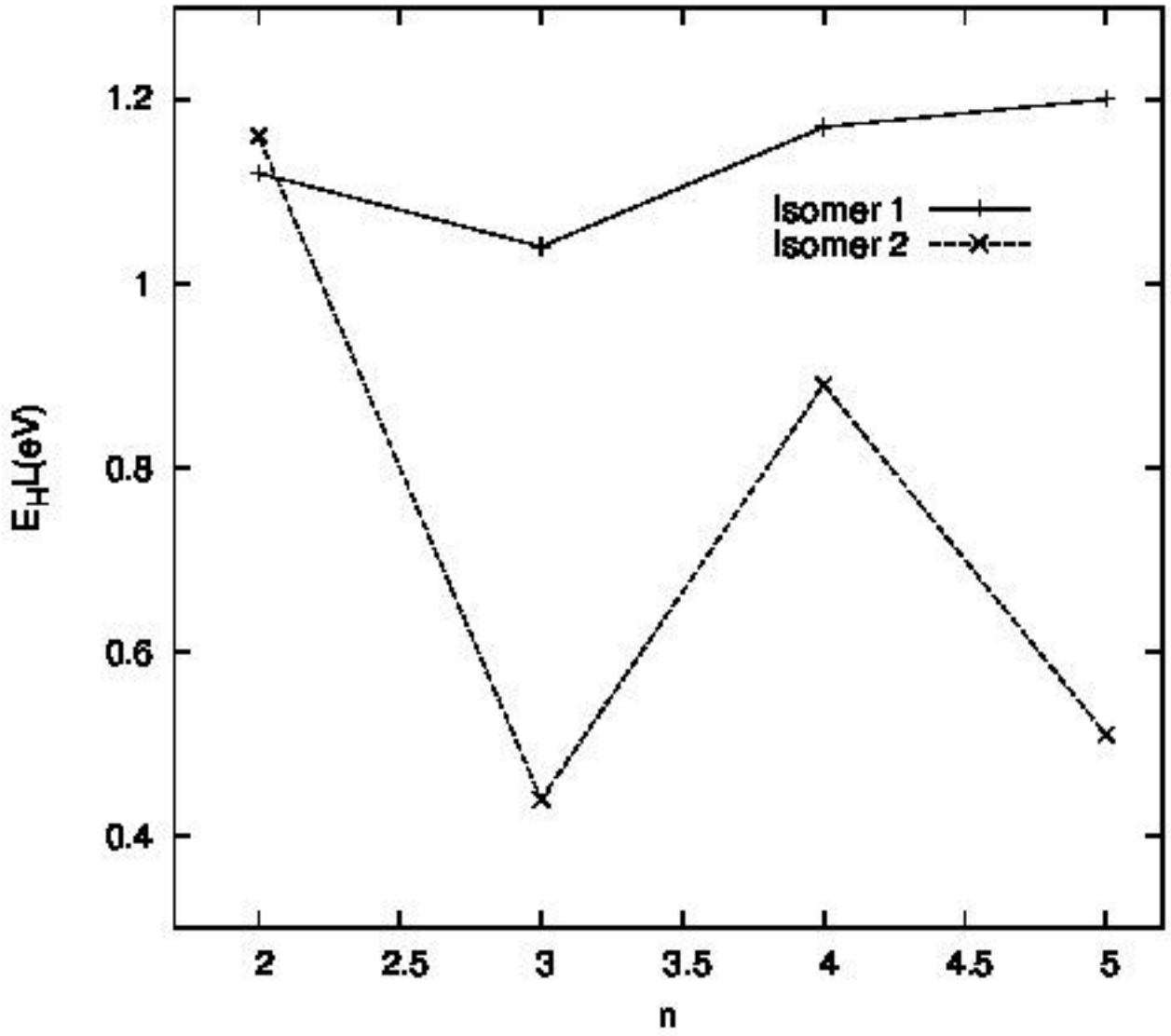

TABLES

Table 1. Bond information for the isolated Au_4 nanocluster (planar diamond) and $C_2H_4S_2H_2$.
Values of the electron density (ρ), its Laplacian ($\nabla^2\rho$) at the corresponding bond critical point (BCP in red in Figure 3(a)) are shown in a.u.. The bond distance Re is also shown (in Å). Bader charges (a.u.) are shown in parenthesis.

Au_4				
Interaction		ρ (r)	∇^2 ρ(r)	R_e
Au-Au'	Au1 (-0.140) - Au2 (0.138)	0.055	0.129	2.713
	Au1 (-0.140) - Au3 (0.140)	0.055	0.128	2.716
	Au2 (0.138) - Au3 (0.140)	0.060	0.153	2.650
	Au3 (0.140) - Au4 (-0.138)	0.055	0.129	2.713
	Au2 (0.138) -Au4 (-0.138)	0.055	0.129	2.711
HS-C_2H_4-S'H'				
Interaction		ρ (r)	∇^2 ρ(r)	R_e
C-C	C1 (-0.027) -C2 (-0.027)	0.238	-0.494	1.523
S-C	S1 (-0.026) -C1 (-0.027)	0.162	-0.186	1.848
	S'2 (-0.026) -C2 (-0.027)	0.162	-0.186	1.848
S-H	S1 (-0.026) -H1 (-0.018)	0.201	-0.469	1.359
	S'2 (-0.026) -H2 (-0.018)	0.201	-0.469	1.359

Table 2. Bond information for the cluster comlexes complexes Au_4-S-C_nH_{2n}-S'-Au_4' (n=2-5). Values of the electron density (ρ), its Laplacian ($\nabla^2\rho$) at the corresponding bond critical point (BCP in red in Figure 3(b)-(e)) are shown in a.u.. The bond distance R_e is also shown (in Å). Bader charges (a.u.) are shown in parenthesis. The bond information for the S-Au interface can be seen in Table 3.

	Au_4-S-C_2H_4-S'-Au'_4								**Au_4-S-C_3H_6-S'-Au'_4**							
Interaction	**ISOMER 1**				**ISOMER 2**				**ISOMER 1**				**ISOMER 2**			
		ρ (r)	∇^2 ρ(r)	R_e		ρ (r)	∇^2 ρ(r)	R_e		ρ (r)	∇^2 ρ(r)	R_e		ρ (r)	∇^2 ρ(r)	R_e
Au-Au'	Au1 (-0.121) - Au2 (0.01)	0.054	0.129	2.718	Au1 (-0.117) - Au2 (0.108)	0.062	0.135	2.644	Au1 (-0.135) - Au2 (0.022)	0.055	0.130	2.711	Au1 (0.095) - Au3 (-0.038)	0.055	0.133	2.710
	Au1 (-0.121) - Au3 (0.118)	0.062	0.136	2.642	Au1 (-0.117) - Au3 (-0.007)	0.054	0.129	2.715	Au1 (-0.135) - Au3 (0.116)	0.061	0.134	2.651	Au3 (-0.038) - Au2 (-0.100)	0.056	0.135	2.695
	Au2 (0.01) - Au3 (0.118)	0.048	0.118	2.776	Au2 (0.108) - Au3 (-0.007)	0.048	0.118	2.777	Au2 (0.022) -Au4 (-0.041)	0.058	0.138	2.679	Au2 (-0.100) - Au4 (0.255)	0.059	0.127	2.673
	Au2 (0.01) - Au4 (0.036)	0.057	0.137	2.691	Au3 (-0.007) - Au4 (0.043)	0.057	0.137	2.689	Au2 (0.022) -Au3 (0.116)	0.051	0.128	2.744	Au3 (-0.038) - Au4 (0.255)	0.051	0.117	2.774
	Au'5 (0.042) - Au'7 (0.000)	0.057	0.137	2.689	Au'5 (0.039) - Au'7 (-0.003)	0.057	0.137	2.689	Au'5 (0.103) -Au'6 (-0.028)	0.049	0.108	2.776	Au'6 (0.102) - Au'7 (-0.129)	0.062	0.135	2.645
	Au'6 (0.102) - Au'7 (0.000)	0.048	0.117	2.788	Au'6 (0.108) - Au'7 (-0.003)	0.048	0.118	2.777	Au'6 (-0.028) - Au'7 (-0.019)	0.047	0.110	2.799	Au'7 (-0.129) - Au'8 (-0.003)	0.054	0.129	2.716

	Au'7 (0.000) - Au'8 (-0.114)	0.054	0.130	2.713	Au'7 (-0.003) - Au'8 (-0.118)	0.054	0.129	2.715	Au'7 (-0.019) - Au'8 (-0.019)	0.046	0.107	2.815	Au'6 (0.102) - Au'8 (-0.003)	0.048	0.118	2.776
	Au'6 (0.102) - Au'8 (-0.114)	0.062	0.135	2.644	Au'6 (0.108) - Au'8 (-0.118)	0.062	0.135	2.644	Au'6 (-0.028) - Au'8 (-0.019)	0.053	0.127	2.732	Au'5 (0.035) - Au'8 (-0.003)	0.057	0.137	2.689
									Au'5 (0.103) -Au'8 (-0.019)	0.053	0.116	2.731				
									Au'5 (0.103) -Au'7 (-0.019)	0.047	0.106	2.803				
C-C	C1 (-0.053) - C2 (-0.033)	0.239	-0.499	1.520	C1 (-0.047) - C2 (-0.040)	0.239	-0.498	1.520	C1 (-0.044) - C2 (0.031)	0.238	-0.491	1.523	C2 (0.043) - C3 (-0.043)	0.229	-0.449	1.538
									C2 (0.031) - C3 (-0.063)	0.238	-0.492	1.524	C1 (-0.087) - C2 (0.043)	0.239	-0.498	1.517
S-C	S1 (-0.092) - C1 (-0.053)	0.158	-0.167	1.861	S1 (-0.088) - C1 (-0.047)	0.158	-0.167	1.861	S1 (0.010) - C1 (-0.044)	0.159	-0.172	1.861	S'2 (-0.073) - C3 (-0.043)	0.160	-0.173	1.856
	S'2 (-0.101) - C2 (-0.033)	0.159	-0.169	1.859	S'2 (-0.093) - C2 (-0.040)	0.158	-0.167	1.861	S'2 (-0.082) - C3 (-0.063)	0.160	-0.173	1.856				
Others									S1 (0.010)	0.042	0.065	2.731	Au4 (0.255)	0.114	0.086	2.108

								- S'2 (-0.082)				- C1 (-0.087)				
	Au_4-S-C_4H_8-S'-Au'_4							**Au_4-S-C_5H_{10}-S'-Au'_4**								
Interaction	**ISOMER 1**				**ISOMER 2**			**ISOMER 1**				**ISOMER 2**				
Au-Au'		ρ (r)	∇^2 ρ(r)	R_e		ρ (r)	∇^2 ρ(r)	R_e		ρ (r)	∇^2 ρ(r)	R_e		ρ (r)	∇^2 ρ(r)	R_e
	Au1 (-0.010) - Au2 (-0.126)	0.054	0.129	2.715	Au1 (-0.073)- Au2 (0.000)	0.052	0.122	2.747	Au1 (-0.125) - Au2 (-0.017)	0.054	0.129	2.718	Au1 (0.019) -Au2 (-0.086)	0.061	0.151	2.650
	Au1 (-0.010) - Au3 (0.031)	0.062	0.135	2.645	Au1 (-0.073)- Au4 (0.099)	0.045	0.102	2.820	Au1 (-0.125) - Au3 (0.115)	0.062	0.136	2.643	Au1 (0.019) -Au3 (-0.081)	0.061	0.151	2.648
	Au2 (-0.126) - Au4 (0.103)	0.057	0.137	2.689	Au1 (-0.073)- Au3 (0.065)	0.043	0.099	2.861	Au2 (-0.017) - Au3 (0.115)	0.048	0.117	2.781	Au2 (-0.086) -Au4 (0.139)	0.050	0.114	2.764
	Au3 (0.031) -Au2 (-0.126)	0.048	0.117	2.783	Au3 (0.065)- Au4 (0.099)	0.052	0.112	2.746	Au2 (-0.017) - Au4 (0.024)	0.057	0.137	2.689	Au3 (-0.081) -Au4 (0.139)	0.050	0.114	2.763
	Au'5 (0.035) -Au'7 (-0.002)	0.057	0.137	2.689	Au3 (0.065)- Au2 (0.000)	0.056	0.135	2.702	Au'7 (-0.013) - Au'6 (0.116)	0.048	0.116	2.784	Au1 (0.019) -Au4 (0.139)	0.052	0.113	2.739
	Au'6 (0.099) -Au'7 (-0.002)	0.048	0.116	2.785	Au2 (0.000)- Au4 (0.099)	0.050	0.109	2.766	Au'7 (-0.013) - Au'8 (-0.123)	0.054	0.128	2.720	Au'5 (0.084) -Au'6 (-0.043)	0.046	0.104	2.806
	Au'6 (0.099) -Au'8	0.062	0.135	2.644	Au'6 (0.093)- Au'8 (-	0.046	0.104	2.805	Au'6 (0.116)- Au'8 (-	0.062	0.136	2.642	Au'5 (0.084) -Au'7	0.052	0.112	2.745

	(-0.125) Au'8 (-0.125) - Au'7 (-0.002)	0.054	0.129	2.716	0.045) Au'6 (0.093) - Au'7 (-0.026)	0.049	0.108	2.778	0.123) Au'5 (0.030) -Au'7 (-0.013)	0.057	0.137	2.690	(0.076) Au'5 (0.084) - Au'8 (-0.035)	0.049	0.109	2.774
					Au'6 (0.093) - Au'5 (0.067)	0.052	0.111	2.749					Au'6 (-0.043) -Au'7 (0.076)	0.054	0.130	2.720
					Au'5 (0.067) - Au'7 (-0.026)	0.055	0.132	2.715					Au'6 (-0.043)- Au'8 (-0.035)	0.041	0.095	2.880
					Au'5 (0.067) - Au'8 (-0.045)	0.054	0.128	2.725					Au'8 (-0.035)- Au'7 (0.076)	0.054	0.130	2.721
					Au'7 (-0.026) - Au'8 (-0.045)	0.041	0.095	2.882								
C-C	C1 (-0.051) - C2 (0.027)	0.236	-0.484	1.527	C1 (-0.047) - C2 (0.046)	0.236	-0.484	1.527	C1 (-0.057) - C2 (0.038)	0.237	-0.488	1.525	C1 (-0.062) -C2 (0.030)	0.236	-0.484	1.528
	C2 (0.027) -C3 (0.028)	0.230	-0.458	1.537	C2 (0.046) - C3 (0.044)	0.231	-0.462	1.536	C2 (0.038) -C3 (0.032)	0.235	-0.482	1.530	C2 (0.030) -C3 (0.016)	0.235	-0.483	1.530
	C3 (0.028) -C4 (-0.042)	0.236	-0.483	1.527	C3 (0.044) - C4 (-0.052)	0.236	-0.484	1.527	C3 (0.032) -C4 (0.026)	0.235	-0.482	1.530	C3 (0.016) -C4 (0.038)	0.235	-0.482	1.530
									C4	0.237	-	1.525	C4	0.235	-	1.529

									(0.026) -C5 (-0.042)		0.488		(0.038) -C5 (-0.042)		0.481	
S-C	S1 (-0.079) - C1 (-0.051)	0.160	-0.174	1.857	S1 (-0.153) - C1 (-0.047)	0.160	-0.175	1.854	S1 (-0.084) - C1 (-0.057)	0.158	-0.169	1.862	S1 (-0.063)- C1 (-0.062)	0.161	-0.179	1.851
	C4 (-0.042) - S'2 (-0.088)	0.160	-0.174	1.857	S'2 (-0.140)- C4 (-0.052)	0.160	-0.174	1.854	S'2 (-0.106) - C5 (-0.042)	0.159	-0.170	1.861	S'2 (-0.141) - C5 (-0.042)	0.159	-0.172	1.857

Table 3. The same bond information as shown in Table 2 for the S-Au bonds separated according to the bonding classification of Figure 2. The S-Au bonds of the S-Au(i) bonding type are divided into two sets: short and large bonds.

Types of bonding between S-Au	Optimized structures of the lowest-energy		Bader Charges	ρ (r)	∇^2 ρ(r)	R_e
i - Short bond	Au_4-S-C_2H_4-S'-Au'_4	ISOMER 1	Au3 (0.118) - S1 (-0.092)	0.090	0.161	2.380
			Au'6 (0.102) - S'2 (-0.101)	0.090	0.159	2.378
		ISOMER 2	Au2 (0.108) - S1 (-0.088)	0.090	0.159	2.377
			Au'6 (0.108) - S'2 (-0.093)	0.090	0.159	2.377
	Au_4-S-C_3H_6-S'-Au'_4	ISOMER 1	Au3 (0.116) - S1 (0.010)	0.091	0.170	2.372
		ISOMER 2	Au'6 (0.102) - S'2 (-0.073)	0.090	0.159	2.378
	Au_4-S-C_4H_8-S'-Au'_4	ISOMER 1	Au3 (0.031) - S1 (-0.079)	0.090	0.158	2.379
			Au'6 (0.099) -S'2 (-0.088)	0.090	0.158	2.380
	Au_4-S-C_5H_{10}-S'-Au'_4	ISOMER 1	Au3 (0.115) - S1 (-0.084)	0.090	0.159	2.378
			Au'6 (0.116) - S'2 (-0.106)	0.090	0.159	2.377
i - Large bond	Au_4-S-C_2H_4-S'-Au'_4	ISOMER 1	Au4 (0.036) - S1 (-0.092)	0.081	0.142	2.433
			Au'5 (0.042) - S'2 (-0.101)	0.080	0.142	2.439
		ISOMER 2	Au4 (0.043) - S1 (-0.088)	0.080	0.143	2.437

			Au'5 (0.039) - S'2 (-0.093)	0.080	0.142	2.439
	Au_4-S-C_3H_6-S'-Au'_4	ISOMER 1	Au4 (-0.041) - S1 (0.010)	0.073	0.116	2.493
		ISOMER 2	Au'5 (0.035) - S'2 (-0.073)	0.081	0.142	2.431
	Au_4-S-C_4H_8-S'-Au'_4	ISOMER 1	Au4 (0.103) - S1 (-0.079)	0.082	0.142	2.430
			Au'5 (0.035) -S'2 (-0.088)	0.081	0.142	2.431
	Au_4-S-C_5H_{10}-S'-Au'_4	ISOMER 1	Au4 (0.024) - S1 (-0.084)	0.082	0.141	2.430
			Au'5 (0.030) - S'2 (-0.106)	0.082	0.141	2.429
ii	Au_4-S-C_3H_6-S'-Au'_4	ISOMER 1	Au'5 (0.103) - S'2 (-0.082)	0.106	0.184	2.288
	Au_4-S-C_4H_8-S'-Au'_4	ISOMER 2	Au4 (0.099) - S1 (-0.153)	0.110	0.165	2.270
			Au'6 (0.093) - S'2 (-0.140)	0.110	0.165	2.271
	Au_4-S-C_5H_{10}-S'-Au'_4	ISOMER 2	Au'5 (0.084) -S'2 (-0.141)	0.110	0.166	2.269
iii	Au_4-S-C_5H_{10}-S'-Au'_4	ISOMER 2	Au4 (0.139) -S1 (-0.063)	0.109	0.180	2.277
iv	Au_4-S-C_3H_6-S'-Au'_4	ISOMER 2	Au1 (0.095) - S1 (-0.254)	0.098	0.130	2.320
			Au4 (0.255) - S1 (-0.254)	0.091	0.118	2.370

Table 4. Total (E), HOMO (E_HOMO), LUMO (E_LUMO) and HOMO-LUMO gap energies in eV.

MOLECULE		ISOMER	E (eV)	E_{HOMO} (Hartee)	E_{LUMO} (Hartee)	HOMO-LUMO gap (eV)
Au_4-S-C_nH_{2n}-S'-Au'_4 (M = 3)	n=2	1	0.000	-0.221	-0.180	1.12
		2	0.001	-0.223	-0.180	1.16
	n=3	1	0.000	-0.208	-0.170	1.04
		2	0.128	-0.207	-0.191	0.44
	n=4	1	0.000	-0.219	-0.176	1.17
		2	1.534	-0.204	-0.171	0.89
	n=5	1	0.000	-0.217	-0.174	1.20
		2	0.996	-0.204	-0.186	0.51
HS-C_nH_{2n}-S'H' (M = 1)	n=2	–	–	-0.210	-0.049	4.38
	n=3	–	–	-0.209	-0.040	4.59
	n=4	–	–	-0.209	-0.033	4.79
	n=5	–	–	-0.207	-0.032	4.78
Au_4	M=1	Trapezoid	0.000	-0.208	-0.172	0.99
	M=3		0.428			

Graphical abstract

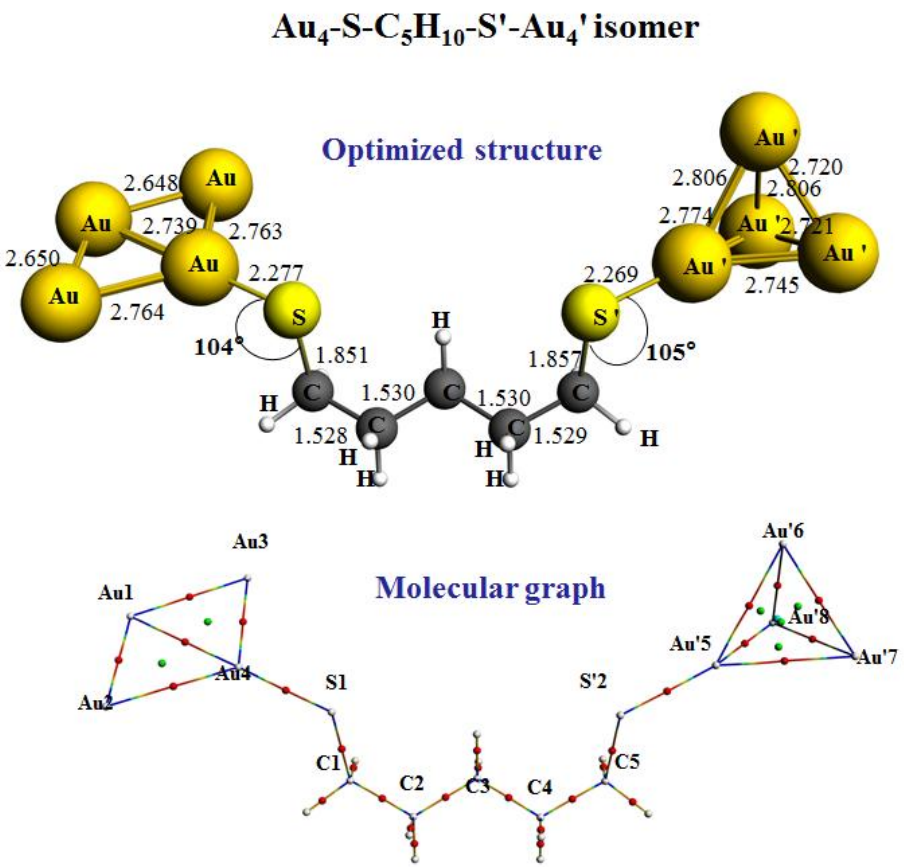

- Theoretical study of cluster complexes Au_4-S-C_nH_{2n}-S'-Au_4'
- The Au-Au and S-S interactions in Au_4-S-C_nH_{2n}-S'-Au_4' are closed shell
- HOMO-LUMO gap has a zigzag behavior with respect to the number of carbon atoms in the complexes Au_4-S-C_nH_{2n}-S'-Au_4'